

The background of the cover is a complex, dark, and highly textured microscopic image of a material structure, possibly a crystal or a composite material. The structure consists of numerous interconnected, angular, and elongated elements that create a dense, intricate pattern. A prominent feature is a bright white square located in the center-left area, which stands out against the dark, blue-tinted background. The overall appearance is that of a highly detailed, three-dimensional microstructure.

Journal of Mechanics of Materials and Structures

BURMISTER'S PROBLEM EXTENDED TO A MICROSTRUCTURED LAYER

Thanasis Zisis

Volume 13, No. 2

March 2018



BURMISTER'S PROBLEM EXTENDED TO A MICROSTRUCTURED LAYER

THANASIS ZISIS

The problem of calculating the displacement and stress field in a layered elastic system loaded on its surface by a certain pressure distribution often arises in engineering analysis and design, in a number of scientific areas ranging from mechanical engineering to soil mechanics and materials science. The solution of such a problem is very important and was first introduced by Biot (1935) but later it was Burmister who presented a complete solution for the stresses and displacements in a general two layer elastic system in which the lower layer is not necessarily rigid (Burmister 1943; Burmister et al. 1944). His results found great application in the field of civil engineering but nowadays can be extended to the technology of barrier, multilayered and/or functionally coatings. Furthermore, due to the ease of manufacturing and assembly, coatings with micro- or even nano-thickness are pursued by manufacturers as hybrid materials for multifunctional devices but as manufacturing scales reduce progressively, the material microstructure itself can play an important role and size effects can be dominant upon the macroscopic mechanical response of the layer/coating. In this study we focus on the loading of a microstructural layer by a normal point load and we present the corresponding Green's functions by extending the solutions suggested by Burmister et al. in order to introduce into the generated displacement and stress fields the effect of the microstructural characteristics of the layer. In order to incorporate the layer material microstructural characteristics we use an effective generalized continuum theory, that is the couple-stress elasticity, in which the material microstructure is introduced constitutively through a length scale. The presented results suggest deviation from those suggested by Burmister et al. in the context of *classical* elasticity for a *layer of finite thickness* as well as from those suggested by Gourgiotis and Zisis (2016) in the context of couple stress elasticity for a *half-plane*.

1. Introduction

Contact situations occur in a multitude of engineering applications ranging from mechanical and civil engineering to materials science. Many structures are founded in reinforced concrete footings or pads buried at relatively shallow depths beneath the ground surface and large scale contacts take place between the footings and the deformable ground. On the other hand, small scale contacts appear in nano-indentation tests in the area of mechanical engineering and/or material science. In an ideal contact situation between two bodies, either within the context of civil engineering where the footing essentially acts as an indenter that lies upon a deformable body (i.e. the ground) or within the spirit of an indentation experiment where the flat surface of the underlying material is mounted perpendicular to the tip of the indenter, the indenter touches the surface of the material and penetration is performed. The details of such penetration may be interpreted in terms of the stress distribution below the indenter and subsequently the stress distribution within the bodies in contact, the surface displacements, the contact site, etc. Such analysis is crucial

Keywords: micromechanics, couple-stress elasticity, Green's functions, microstructured layers, coatings.

for design purposes in geotechnical and footing engineering, or in the case of material characterization through indentation tests.

Coatings with thickness ranging from micro- to nanometers are currently manufactured as materials for multifunctional devices. Such applications of coatings range from insulators to thermal and corrosion barrier systems. The mechanical properties of such coatings and the observed failure mechanisms are of great interest for design purposes and a very efficient technique in order to extract such mechanical characteristics is the micro- and nano-indentation experiment. Furthermore, material systems that comprise of several layers are usually found in the field of soil mechanics and from structural considerations the problem of calculating the stress and displacement fields within the material system as well as at the layer interface is of great importance.

It is well known that under loading conditions, size effects can be dominant especially when the characteristic lengths of the problems are comparable to the characteristic material length scale which is associated to the materials inherent microstructure. In fact, the macroscopical behavior of most microstructured materials with nonhomogeneous microstructure, like ceramics, composites, cellular materials, foams, masonry, bone tissues, glassy and semicrystalline polymers, is strongly influenced by the microstructural characteristic lengths, especially in the presence of large stress (or strain) gradients [Maranganti and Sharma 2007].

The generalized continuum theories smear-out the material microstructure and enrich the classical continuum with additional material characteristic length scales extending, thus, the range of applicability of the “continuum” concept in an effort to bridge the gap between classical continuum theories and atomic-lattice theories. This approach is very effective since it can be incorporated efficiently into large computations but of course lacks the detailed description of a discrete representation and treats the microstructural length in an average sense [Muki and Sternberg 1965; Poole et al. 1996; Begley and Hutchinson 1998; Nix and Gao 1998; Shu and Fleck 1998; Wei and Hutchinson 2003; Zisis et al. 2014; Zisis 2017; Gourgiotis et al. 2018].

The physical relevance of the material length scale as introduced through generalized continuum theories has been the subject of numerous theoretical and experimental studies. Chen et al. [1998], for example, developed a continuum model for cellular materials and concluded that the continuum description of these materials obeys a gradient elasticity theory of the couple-stress type. In the latter study, the intrinsic material length was identified with the cell size. Tekoglu and Onck [2008] compared the analytical results of various gradient type generalized continuum theories with the computational results of discrete models through a range of basic boundary value problems based on Voronoi representations of cellular microstructures. The analysis they performed, strictly within the elastic regime, assessed the capabilities of generalized continuum theories in capturing size effects in cellular solids and connected the cell size with the microstructural length-scale. Two recent studies [Bigoni and Drugan 2007; Bacca et al. 2013] provide an account of the determination of the couple-stress moduli via homogenization of heterogeneous materials. Finally, Shodja et al. [2013], using *ab initio* DFT calculations, evaluated the characteristic material lengths of the gradient elasticity theory for several fcc and bcc metal crystals.

One effective generalized continuum theory has proved to be that of couple-stress elasticity, also known as Cosserat theory with constrained rotations [Mindlin and Tiersten 1962; Toupin 1964]. In the context of couple-stress elasticity, the strain-energy density and the resulting constitutive relations involve, besides the usual infinitesimal strains, certain strain gradients known as the rotation gradients.

The generalized stress-strain relations for the isotropic case include, in addition to the conventional pair of elastic constants, two new elastic constants, one of which is expressible in terms of a material parameter ℓ that has dimension of [length]. The presence of this length parameter, in turn, implies that the modified theory encompasses the analytical possibility of size effects, which are absent in the classical theory.

The simplest case of a layered system is that of an elastic layer bonded on a rigid base. For a multitude of layered systems, ranging from materials science to soil mechanics, the bonding condition sufficiently describes the interface characteristics. This problem, in the context of classical elasticity, has received attention from several investigators. Marguerre [1931] obtained a solution for the stresses in the layer under plane strain conditions, while Biot [1935] examined both the case of plain strain and axial symmetry with restriction to the calculation of the normal stresses. Biot's work was extended by Pickett [1938], who presented the complete stress and displacement fields under both plane strain and axisymmetric conditions.

A general solution in terms of a two-layer elastic system in which the lower layer is not necessarily rigid was given in [Burmister 1943; Burmister et al. 1944; Burmister 1945a; 1945b]. In [Burmister 1956] this was extended to a complete mathematical solution regarding the stress and displacement fields in a layer bonded on a rigid substrate loaded by a point load. This now classical problem, bearing Burmister's name, finds applications in mechanical and civil engineering as well as materials science. A number of works have followed since, that either extended the classical Burmister's problem to different geometries and different loading conditions but all in the context of classical elasticity [Schiffman 1957; Davis and Taylor 1961; Davis and Poulos 1963; Poulos 1967].

Our purpose is to study the macroscopic response of a bonded layer with microstructural characteristics. For this reason in the present work, we extend the classical work of Burmister and we examine the mechanics under which the presence of a rigid substrate, the finite thickness of the deformable layer as well as the material microstructural characteristics, influence the displacement and stress fields.

The problem under investigation is solved in the frame of couple stress theory and it is anticipated that our results will be essentially intermediate to those of [Burmister 1956] for the case of a layer in the context of classical elasticity and those of [Gourgiotis and Zisis 2016] for the half-plane in the frame of couple-stress theory.

2. Basic equations of couple-stress elasticity in plane-strain

In this section, we summarize the main features of the linearized couple-stress theory of homogeneous and isotropic elastic solids [Mindlin and Tiersten 1962; Koiter 1964a; Koiter 1964b]. An exposition of the theory under plane-strain conditions was given in [Muki and Sternberg 1965], and more recently by [Gourgiotis and Piccolroaz 2014] in the elastodynamic case including micro-inertial effects.

For a body that occupies a domain in the (x, y) -plane under conditions of plane-strain, the equations of equilibrium in the absence of body forces and body moments reduce to

$$\frac{\partial \sigma_{xx}}{\partial x} + \frac{\partial \sigma_{yx}}{\partial y} = 0, \quad \frac{\partial \sigma_{xy}}{\partial x} + \frac{\partial \sigma_{yy}}{\partial y} = 0, \quad \sigma_{xy} - \sigma_{yx} + \frac{\partial m_{xz}}{\partial x} + \frac{\partial m_{yz}}{\partial y} = 0, \quad (1)$$

where $(\sigma_{xx}, \sigma_{xy}, \sigma_{yx}, \sigma_{yy})$ and (m_{xz}, m_{yz}) are the nonvanishing components of the (asymmetric) stress and couple-stress tensors, respectively. The complete solution of (1) admits the following representation in terms of two sufficiently smooth stress functions $\Phi \equiv \Phi(x, y)$ and $\Psi \equiv \Psi(x, y)$ [Mindlin 1963]:

$$\begin{aligned}\sigma_{xx} &= \frac{\partial^2 \Phi}{\partial y^2} - \frac{\partial^2 \Psi}{\partial x \partial y}, & \sigma_{yy} &= \frac{\partial^2 \Phi}{\partial x^2} + \frac{\partial^2 \Psi}{\partial x \partial y}, \\ \sigma_{xy} &= -\frac{\partial^2 \Phi}{\partial x \partial y} - \frac{\partial^2 \Psi}{\partial y^2}, & \sigma_{yx} &= -\frac{\partial^2 \Phi}{\partial x \partial y} + \frac{\partial^2 \Psi}{\partial x^2},\end{aligned}\quad (2)$$

and

$$m_{xz} = \frac{\partial \Psi}{\partial x}, \quad m_{yz} = \frac{\partial \Psi}{\partial y}.\quad (3)$$

Accordingly, the displacement field assumes the following general form:

$$u_x \equiv u_x(x, y), \quad u_y \equiv u_y(x, y), \quad u_z \equiv 0.\quad (4)$$

The governing kinematic relations in the framework of the geometrically linear theory then become:

$$\varepsilon_{xx} = \frac{\partial u_x}{\partial x}, \quad \varepsilon_{yy} = \frac{\partial u_y}{\partial y}, \quad \varepsilon_{xy} = \varepsilon_{yx} = \frac{1}{2} \left(\frac{\partial u_y}{\partial x} + \frac{\partial u_x}{\partial y} \right),\quad (5)$$

$$\omega_z = \frac{1}{2} \left(\frac{\partial u_y}{\partial x} - \frac{\partial u_x}{\partial y} \right), \quad \kappa_{xz} = \frac{\partial \omega_z}{\partial x}, \quad \kappa_{yz} = \frac{\partial \omega_z}{\partial y},\quad (6)$$

where ε is the usual strain tensor, ω_z is the rotation, and $(\kappa_{xz}, \kappa_{yz})$ are the nonvanishing components of the curvature tensor (i.e. the gradient of rotation) expressed in dimensions of $[\text{length}]^{-1}$. For a homogeneous and isotropic couple-stress material the constitutive equations furnish:

$$\begin{aligned}\varepsilon_{xx} &= (2\mu)^{-1}[\sigma_{xx} - \nu(\sigma_{xx} + \sigma_{yy})], & \varepsilon_{yy} &= (2\mu)^{-1}[\sigma_{yy} - \nu(\sigma_{xx} + \sigma_{yy})], \\ \varepsilon_{xy} &= (4\mu)^{-1}(\sigma_{xy} + \sigma_{yx}),\end{aligned}\quad (7)$$

and

$$\kappa_{xz} = (4\mu\ell^2)^{-1}m_{xz}, \quad \kappa_{yz} = (4\mu\ell^2)^{-1}m_{yz},\quad (8)$$

where μ , ν , and ℓ stand for the shear modulus, Poisson's ratio, and characteristic material length of couple-stress theory, respectively [Mindlin and Tiersten 1962].

Further, substitution of (2) and (3) into (7) and (8) results in the compatibility equations for the Mindlin's stress functions:

$$\frac{\partial}{\partial x}(\Psi - \ell^2 \nabla^2 \Psi) = -2(1 - \nu)\ell^2 \nabla^2 \left(\frac{\partial \Phi}{\partial y} \right),\quad (9)$$

$$\frac{\partial}{\partial y}(\Psi - \ell^2 \nabla^2 \Psi) = 2(1 - \nu)\ell^2 \nabla^2 \left(\frac{\partial \Phi}{\partial x} \right),\quad (10)$$

from which, in turn, we obtain the following uncoupled partial differential equations:

$$\nabla^4 \Phi = 0,\quad (11)$$

$$\nabla^2 \Psi - \ell^2 \nabla^4 \Psi = 0.\quad (12)$$

Note that as the quantities ℓ , $\partial \Psi / \partial x$, and $\partial \Psi / \partial y$ tend to zero, the above representation passes over into the classical Airy's representation.

3. Concentrated load at the surface of a bonded layer with microstructure

The definition of a Green's function can be used mathematically to derive solutions to point load problems, either within the elastic body or on its surface. A multitude of Green's functions within the context of classical elasticity are available in the literature for different surface geometries (see e.g., [Green and Zerna 1968]). In a 2D setting, the problem of determining the stress and displacement fields in an isotropic half-plane subjected to a concentrated line load on its surface is the celebrated Flamant–Boussinesq problem. The Flamant–Boussinesq solution of classical elasticity is discussed among others, e.g., by [Love 1952; Fung 1965; Timoshenko and Goodier 1970], and enjoys important applications mainly in Contact Mechanics and Tribology, since it can be used as a building block for the formulation of complicated contact problems (see e.g. [Johnson 1985; Hills and Nowell 1994; Barber 2010]).

In the context of generalized continuum theories, concentrated load problems have been extensively studied suggesting solutions that significantly depart from the predictions of classical elasticity (see for example the works of [Georgiadis and Anagnostou 2008; Gourgiotis and Zisis 2016; Zisis 2017; Gourgiotis et al. 2018]). Regarding the couple-stress theory, [Muki and Sternberg 1965] were the first to derive the asymptotic fields for the stress field in the Flamant–Boussinesq problem while recently full field solutions were presented by [Gourgiotis and Zisis 2016]. Here, we provide a solution for the concentrated load problem at the surface of a microstructured layer in the context of couple stress theory of elasticity which can accordingly be used as the pertinent Green's function for the formulation of the plane contact problems.

Consider a body occupying the half-plane ($-\infty < x < \infty$, $0 \leq y \leq h$) under plane strain conditions subjected to a normal line load P on its surface (see Figure 1). The point of application of the concentrated load is taken as the origin ($x = y = 0$) of a Cartesian rectangular coordinate system. The intensities of the concentrated loads are expressed in dimensions of $[\text{force}][\text{length}]^{-1}$.

Accordingly, the boundary conditions along the surface $y = 0$ become:

$$\sigma_{yy}(x, 0) = -P\delta(x), \quad -\infty < x < \infty, \quad (13)$$

$$\sigma_{yx}(x, 0) = 0, \quad -\infty < x < \infty, \quad (14)$$

$$m_{yz}(x, 0) = 0, \quad -\infty < x < \infty, \quad (15)$$

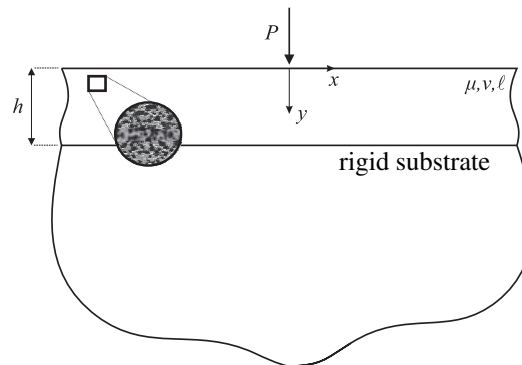


Figure 1. Normal load acting on the surface of an elastic layer of thickness h bonded onto the rigid substrate. This is Burmister's problem (1953) extended to a microstructured layer in the context of couple-stress elasticity.

where $\delta(x)$ is the Dirac delta function. The solution procedure for the case of a tangential load acting on the surface of a half-plane is directly analogous to what will be presented in what follows and is omitted for sake of brevity.

Regarding the boundary conditions at the interface between the microstructured layer and the rigid substrate, we can define two different sets of boundary conditions as follows:

(1) The first set suggests vanishing displacements and rotations as:

$$u_x(x, h) = 0, \quad -\infty < x < \infty, \quad (16)$$

$$u_y(x, h) = 0, \quad -\infty < x < \infty, \quad (17)$$

$$\omega_z(x, h) = 0, \quad -\infty < x < \infty, \quad (18)$$

(2) The second set suggests vanishing displacements and couple stresses m_{yz} as:

$$u_x(x, h) = 0, \quad -\infty < x < \infty, \quad (19)$$

$$u_y(x, h) = 0, \quad -\infty < x < \infty, \quad (20)$$

$$m_{yz}(x, h) = 0, \quad -\infty < x < \infty, \quad (21)$$

Note that the first set of boundary conditions corresponds to an over-constrained version of the classical elasticity solution while the second set of boundary conditions allows for a direct comparison of the current solution with the classical elasticity results.

The problem is attacked with the aid of the Fourier transform on the basis of the stress function formulation summarized earlier. The direct Fourier transform and its inverse are defined by

$$\hat{f}(\xi) = \int_{-\infty}^{\infty} f(x)e^{i\xi x} dx, \quad f(x) = \frac{1}{2\pi} \int_{-\infty}^{\infty} \hat{f}(\xi)e^{-i\xi x} d\xi. \quad (22)$$

The transformation of (11) and (12) through (22) yields the following ODEs for the transformed stress functions:

$$\frac{d^4 \hat{\Phi}}{dy^4} - 2\xi^2 \frac{d^2 \hat{\Phi}}{dy^2} + \xi^4 \hat{\Phi} = 0, \quad (23)$$

$$\ell^2 \frac{d^4 \hat{\Psi}}{dy^4} - (1 + 2\ell^2 \xi^2) \frac{d^2 \hat{\Psi}}{dy^2} + \xi^2 (1 + \ell^2 \xi^2) \hat{\Psi} = 0. \quad (24)$$

The transformed stresses and couple-stresses become

$$\begin{aligned} \hat{\sigma}_{xx} &= \frac{d^2 \hat{\Phi}}{dy^2} + i\xi \frac{d\hat{\Psi}}{dy}, & \hat{\sigma}_{yy} &= -\xi^2 \hat{\Phi} - i\xi \frac{d\hat{\Psi}}{dy}, \\ \hat{\sigma}_{yx} &= i\xi \frac{d\hat{\Phi}}{dy} - \xi^2 \hat{\Psi}, & \hat{\sigma}_{xy} &= i\xi \frac{d\hat{\Phi}}{dy} - \frac{d^2 \hat{\Psi}}{dy^2}, \end{aligned} \quad (25)$$

$$\hat{m}_{xz} = -i\xi \hat{\Psi}, \quad \hat{m}_{yz} = \frac{d\hat{\Psi}}{dy}, \quad (26)$$

whereas the displacements become

$$\begin{aligned} \hat{u}_x &= \frac{1}{2\mu\xi} \left(i(1-\nu) \frac{d^2\hat{\Phi}}{dy^2} - \xi \frac{d\hat{\Psi}}{dy} + i\nu\xi^2\hat{\Phi} \right), \\ \hat{u}_y &= \frac{1}{2\mu\xi^2} \left((1-\nu) \frac{d^3\hat{\Phi}}{dy^3} - (2-\nu)\xi^2 \frac{d\hat{\Phi}}{dy} - i\xi^3\hat{\Psi} \right). \end{aligned} \tag{27}$$

The governing equations (23) and (24) have the following general solution:

$$\hat{\Phi}(\xi, y) = [C_1(\xi) + yC_2(\xi)]e^{-|\xi|y} + [C_3(\xi) + yC_4(\xi)]e^{|\xi|y}, \tag{28}$$

$$\hat{\Psi}(\xi, y) = B_1(\xi)e^{-|\xi|y} + B_2(\xi)e^{-\gamma y} + B_3(\xi)e^{\xi y} + B_4(\xi)e^{\gamma y}, \tag{29}$$

where $\gamma \equiv \gamma(\xi) = (1/\ell^2 + \xi^2)^{1/2}$.

Enforcing the boundary conditions (13)–(15) for the layer surface and (16)–(18) or (19)–(21) for the base of the layer, and the compatibility equations (9) and (10), we obtain a system of eight equations (written in matrix form in Appendix) which are solved for the unknown functions $B_i(\xi)$ and $C_i(\xi)$ with $i = 1, \dots, 4$. Auxiliary conditions are obtained through the compatibility equations as:

$$B_1(\xi) = -4i\ell^2(1-\nu)\xi C_2(\xi), \tag{30}$$

$$B_3(\xi) = -4i\ell^2(1-\nu)\xi C_4(\xi). \tag{31}$$

Upon substitution of the functions $B_i(\xi)$, $C_i(\xi)$ into (27)–(29), and utilizing the fact that $\hat{u}_x(x, \xi)$, $\hat{\omega}_z(x, \xi)$ and $\hat{u}_y(x, \xi)$ are odd, odd and even functions of ξ , respectively, the components of the transformed displacement and rotation field become:

$$u_x(x, y) = \frac{-i}{\pi} \int_0^\infty \hat{u}_x(\xi, y) \sin(\xi x) d\xi, \tag{32}$$

$$u_y(x, y) = \frac{1}{\pi} \int_0^\infty \hat{u}_y(\xi, y) \cos(\xi x) d\xi, \tag{33}$$

$$\omega_z(x, y) = \frac{-i}{\pi} \int_0^\infty \hat{\omega}_z(\xi, y) \sin(\xi x) d\xi, \tag{34}$$

while under similar considerations, the stresses and couple stresses read:

$$\sigma_{xx}(x, y) = \frac{1}{\pi} \int_0^\infty \hat{\sigma}_{xx}(\xi, y) \cos(\xi x) d\xi, \tag{35}$$

$$\sigma_{yy}(x, y) = \frac{1}{\pi} \int_0^\infty \hat{\sigma}_{yy}(\xi, y) \cos(\xi x) d\xi, \tag{36}$$

$$\sigma_{xy}(x, y) = \frac{-i}{\pi} \int_0^\infty \hat{\sigma}_{xy}(\xi, y) \sin(\xi x) d\xi, \tag{37}$$

$$\sigma_{yx}(x, y) = \frac{-i}{\pi} \int_0^\infty \hat{\sigma}_{yx}(\xi, y) \sin(\xi x) d\xi, \tag{38}$$

$$m_{xz}(x, y) = \frac{1}{\pi} \int_0^\infty \hat{m}_{xz}(\xi, y) \cos(\xi x) d\xi, \tag{39}$$

$$m_{yz}(x, y) = \frac{-i}{\pi} \int_0^\infty \hat{m}_{yz}(\xi, y) \sin(\xi x) d\xi. \tag{40}$$

In fact for the same problem, in terms of loading conditions and in the context of couple stress theory, the half-plane solution for the displacement and rotation field reads thus [Gourgiotis and Zisis 2016]:

$$u_x(x, y) = \frac{P}{2\mu\pi} \int_0^\infty \frac{4\ell^2(1-\nu)\xi^2\gamma e^{-\gamma y} + (\gamma(y\xi - 1 + 2\nu) - 4\ell^2(1-\nu)\xi^3)e^{-\xi y}}{\xi(\gamma - 4(1-\nu)\ell^2\xi^2(\xi - \gamma))} \sin(\xi x) d\xi, \quad (41)$$

$$u_y(x, y) = \frac{P}{2\mu\pi} \int_0^\infty \frac{4\ell^2(1-\nu)\xi^3 e^{-\gamma y} + (\gamma(y\xi + 2(1-\nu)) - 4\ell^2(1-\nu)\xi^3)e^{-\xi y}}{\xi(\gamma - 4(1-\nu)\ell^2\xi^2(\xi - \gamma))} \cos(\xi x) d\xi, \quad (42)$$

$$\omega_z(x, y) = \frac{P}{2\mu\pi} \int_0^\infty \frac{e^{-y(\gamma+\xi)}(1-\nu)(e^{y\xi}\ell^2\xi(\gamma-\xi)(\gamma+\xi) - e^{y\gamma}\gamma)}{\gamma - 4\ell^2\gamma(-1+\nu)\xi^2 + 4\ell^2(-1+\nu)\xi^3} \sin(\xi x) d\xi, \quad (43)$$

while the stresses and couple-stresses follow as:

$$\sigma_{xx}(x, y) = \frac{P}{\pi} \int_0^\infty \frac{e^{-y(\gamma+\xi)}(e^{y\gamma}(\gamma - y\gamma\xi + 4\ell^2(1-\nu)\xi^3) - 4e^{y\xi}\ell^2\gamma(1-\nu)\xi^2)}{4\ell^2(1-\nu)\xi^3 - \gamma(1 + 4\ell^2(1-\nu)\xi^2)} \cos(\xi x) d\xi, \quad (44)$$

$$\sigma_{yy}(x, y) = \frac{P}{\pi} \int_0^\infty \frac{e^{-y(\gamma+\xi)}(4e^{y\xi}\ell^2\gamma(1-\nu)\xi^2 + e^{y\gamma}(\gamma + y\gamma\xi - 4\ell^2(1-\nu)\xi^3))}{4\ell^2(1-\nu)\xi^3 - \gamma(1 + 4\ell^2(1-\nu)\xi^2)} \cos(\xi x) d\xi, \quad (45)$$

$$\sigma_{xy}(x, y) = \frac{P}{\pi} \int_0^\infty \frac{e^{-y(\gamma+\xi)}\xi(4e^{y\xi}\ell^2\gamma^2(1-\nu) + e^{y\gamma}(y\gamma - 4\ell^2(1-\nu)\xi^2))}{4\ell^2(1-\nu)\xi^3 - \gamma(1 + 4\ell^2(1-\nu)\xi^2)} \sin(\xi x) d\xi, \quad (46)$$

$$\sigma_{yx}(x, y) = \frac{P}{\pi} \int_0^\infty \frac{e^{-y(\gamma+\xi)}(4e^{y\xi}\ell^2(1-\nu)\xi^2 + e^{y\gamma}(y\gamma - 4\ell^2(1-\nu)\xi^2))}{4\ell^2(1-\nu)\xi^3 - \gamma(1 + 4\ell^2(1-\nu)\xi^2)} \sin(\xi x) d\xi, \quad (47)$$

$$m_{xz}(x, y) = \frac{P}{\pi} \int_0^\infty \frac{4e^{-y(\gamma+\xi)}(1-\nu)(e^{y\xi}\xi - e^{y\gamma}\gamma)\ell^2\xi}{\gamma(1 + 4\ell^2(1-\nu)\xi^2) - 4\ell^2(1-\nu)\xi^3} \cos(\xi x) d\xi, \quad (48)$$

$$m_{yz}(x, y) = \frac{P}{\pi} \int_0^\infty \frac{4e^{-y(\gamma+\xi)}(1-\nu)(e^{y\gamma} - e^{y\xi})\gamma\ell^2\xi}{\gamma(1 + 4\ell^2(1-\nu)\xi^2) - 4\ell^2(1-\nu)\xi^3} \sin(\xi x) d\xi. \quad (49)$$

In classical elasticity, for a layer of finite thickness h loaded on its surface by a normal load, the corresponding to (32) and (33) for $y = 0$ are given as:

$$u_x^{\text{class-layer}}(x, 0) = \frac{P}{2\mu\pi} \int_0^\infty \frac{(3-2\nu(5-4\nu)+2h^2\xi^2-(3-2(5-4\nu)\nu) \cosh(2h\xi))}{\xi(5-4\nu(3-2\nu)+2h^2\xi^2+(3-4\nu) \cosh(2h\xi))} \sin(\xi x) d\xi, \quad (50)$$

$$u_y^{\text{class-layer}}(x, 0) = \frac{P}{\mu\pi} \int_0^\infty \frac{(1-\nu)((3-4\nu) \sinh(2h\xi))}{\xi(5-4\nu(3-2\nu)+2h^2\xi^2+(3-4\nu) \cosh(2h\xi))} \sin(\xi x) d\xi, \quad (51)$$

$$\omega_z^{\text{class-layer}}(x, 0) = \frac{P}{\mu\pi} \int_0^\infty \frac{(1-\nu)(2h\xi - (3-4\nu) \sinh(2h\xi))}{\mu(5-4\nu)(3-2\nu)+2h^2\xi^2+(3-4\nu) \cosh(2h\xi))} \sin(\xi x) d\xi, \quad (52)$$

while the stress field at the interface ($y = h$) reads:

$$\sigma_{yy}^{\text{class-layer}}(x, h) = \frac{P}{\pi} \int_0^\infty \frac{-4(1-\nu)(2(1-\nu) \cosh(h\xi) + h\xi \sinh(h\xi))}{5-4\nu(3-2\nu)+2h^2\xi^2+(3-4\nu) \cosh(2h\xi)} \cos(\xi x) d\xi, \quad (53)$$

$$\sigma_{yx}^{\text{class-layer}}(x, h) = \frac{P}{\pi} \int_0^\infty \frac{4(1-\nu)(h\xi \cosh(h\xi) - (1-2\nu) \sinh(h\xi))}{5-4\nu(3-2\nu)+2h^2\xi^2+(3-4\nu) \cosh(2h\xi)} \sin(\xi x) d\xi. \quad (54)$$

The preceding equations for the half-plane reduce to the following set:

$$u_x^{\text{class}}(x, 0) = -\frac{P(1-2\nu)}{4\mu} \text{sgn}(x), \quad (55)$$

$$u_y^{\text{class}}(x, 0) = \frac{-P(1-\nu)}{\pi\mu} \log(x), \quad (56)$$

$$\omega_z^{\text{class}}(x, 0) = \frac{P(1-\nu)}{\pi\mu x}, \quad (57)$$

$$\sigma_{yy}^{\text{class}}(x, y) = -\frac{2Py^3}{\pi(x^2+y^2)^2}, \quad (58)$$

$$\sigma_{yx}^{\text{class}}(x, y) = -\frac{2Pxy^2}{\pi(x^2+y^2)^2}. \quad (59)$$

The asymptotic behavior of the tangential and normal displacements in the context of couple-stress elasticity for a half-plane was examined near the point of the application of the concentrated load by [Gourgiotis and Zisis 2016] by employing theorems of the Abel–Tauber type and examining the behavior of the transformed solutions for the displacements as $\xi \rightarrow \infty$. It was shown that

$$u_x^{\text{asympt}}(x, y) = \frac{P}{2\mu\pi(3-2\nu)} \left[-(1-2\nu) \frac{xy}{r^2} + \tan^{-1}\left(\frac{x}{y}\right) \right], \quad (60)$$

$$u_y^{\text{asympt}}(x, y) = -\frac{P}{2\mu\pi(3-2\nu)} \left[(1-2\nu) \frac{y^2}{r^2} + 2(1-\nu) \log(r) \right], \quad (61)$$

with $r = (x^2 + y^2)^{1/2}$.

As a final comment we note that examination of the transformed normal displacements for the case of the layer and regardless of the theory employed, suggests that $u_y(x, 0) \rightarrow 0$ as $x \rightarrow 0$. In marked difference, for the case of the half-plane, the integrand in (33) behaves as $\hat{u}_y(\xi, y) = O(\xi^{-1})$ for $\xi \rightarrow 0$, and, thus, $u_y(x, y)$ exhibits a logarithmic behavior as $x \rightarrow \infty$. It can be furthermore shown that regardless again of the theory employed, the strains remain singular and behave as $\varepsilon_{ij} = O(x^{-1})$ for $x \rightarrow 0$. However, in marked contrast to the classical elasticity theory, in the couple stress theory, the rotation is bounded at the point of application of the load. It is noted that in the classical theory the rotation is singular, exhibiting $O(x^{-1})$ singular behavior as $x \rightarrow 0$, see (57).

4. Results and discussion

Results regarding the behavior of the surface ($y = 0$) in terms of displacement and rotation of a layer loaded by a normal load in the frame of classical as well as in couple-stress elasticity are presented in Figures 2–5. Furthermore, full-field results are presented in terms of contours in Figures 6–8. Normalization of the problem suggests that the distance from the point of the application of the load should be normalized with the thickness of the layer (x/h), the normal and tangential displacements should be normalized as $\mu u_x/P$, $\mu u_y/P$ respectively and the rotations should be normalized as $\mu h \omega_z/P$.

We begin the discussion from the case of the layer in the context of classical elasticity. In Figure 2 we present the displacements and rotation of the layer's surface ($y = 0$) for two different values of the

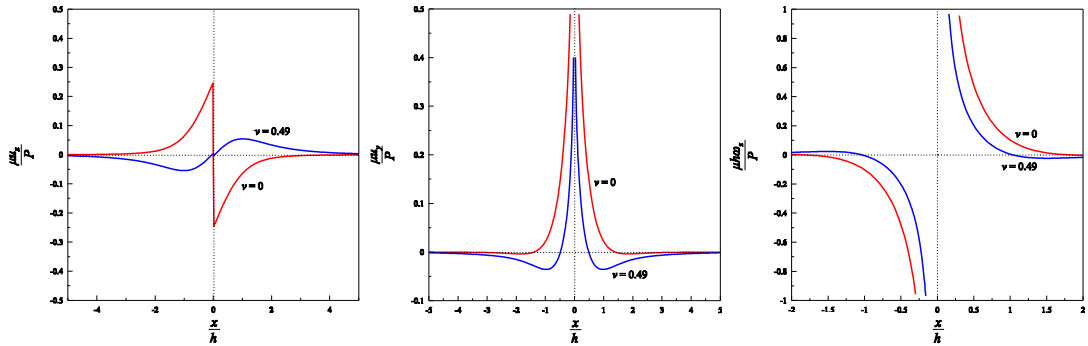


Figure 2. Behavior of the surface of a layer of thickness h under the action of a normal point load in the frame of classical elasticity. Tangential displacement $\mu u_x/P$ (left), normal displacement $\mu u_y/P$ (middle) and rotation angle $\mu h\omega_z/P$ (right) are presented as functions of the normalized distance x/h from the point of the application of the load P for two different Poisson's ratios: $\nu = 0$ (red) and $\nu = 0.49$ (blue).

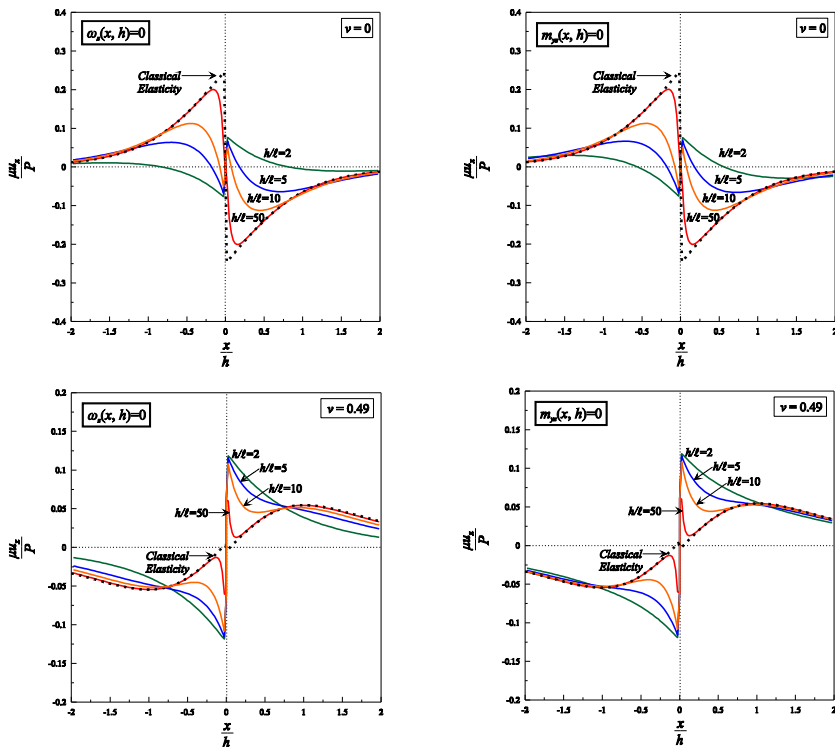


Figure 3. Behavior of the surface of a layer of thickness h under the action of a normal point load in the frame of couple stress elasticity. The normalized tangential displacements $\mu u_x/P$ are plotted versus the normalized distance x/h from the point of the application of the load P for two Poisson's ratios (top, $\nu = 0$; bottom, $\nu = 0.49$) and two different boundary conditions at the interface: either $\omega_z(x, h) = 0$ (left) or $m_{yz}(x, h) = 0$ (right). The classical elasticity solution for the layer of thickness h is superimposed.

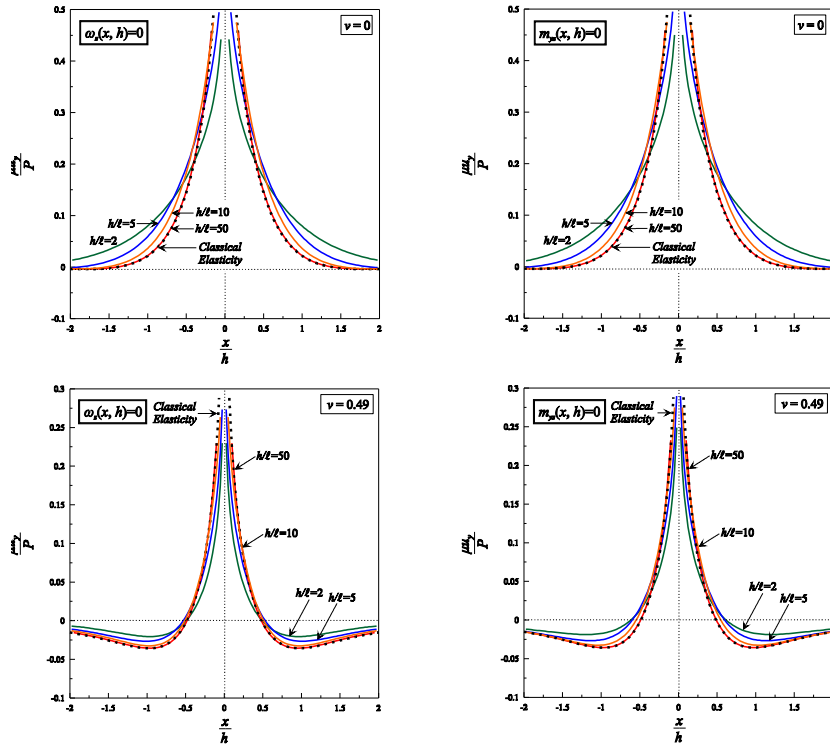


Figure 4. Behavior of the surface of a layer of thickness h under the action of a normal point load in the frame of couple stress elasticity. The normalized normal displacements $\mu u_y/P$ are plotted versus the normalized distance x/h from the point of the application of the load P for two Poisson's ratios (top, $\nu = 0$; bottom, $\nu = 0.49$) and two different boundary conditions at the interface: either $\omega_z(x, h) = 0$ (left) or $m_{yz}(x, h) = 0$ (right). The classical elasticity solution for the layer of thickness h is superimposed.

Poisson's ratio. The normalization proposed suggests that in the case of classical elasticity the curves are unique for a fixed value of Poisson's ratio. The discontinuous tangential displacement and the singular behavior of the normal displacement at the point of the application of the load are the same as in the case of the half-plane ($h \rightarrow \infty$) but as we move further from the point of the application of the load the normal displacements decay and can be seen that essentially for $x/h \geq 5$ they vanish for both values of Poisson's ratio. It is further noted that for almost incompressible material the surface laterally to the point of the application of the load is piling-up (Figure 2, middle) while the rotation, being unbounded at the point of application of the load, increases for decreasing Poisson's ratio.

Next, we move to the case of the surface of the layer in the frame of couple-stress elasticity (Figures 3–8). Here we present the normal and tangential displacements as well as the rotation for selected values of Poisson's ratio. The results are shown for two different boundary conditions at the layer/rigid substrate interface. We conclude that the effect of the two different sets of boundary conditions at the bottom of the layer is of minor importance upon the displacements and the rotation at the surface. As expected as the layer thickness increases the effect decays.

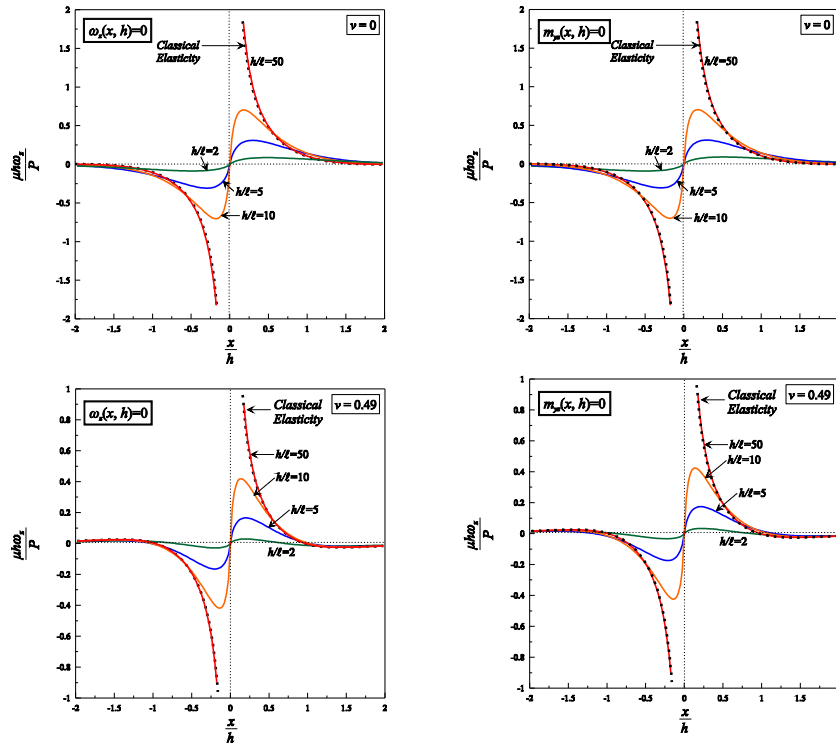


Figure 5. Behavior of the surface of a layer of thickness h under the action of a normal point load in the frame of couple stress elasticity. The normalized rotation $\mu h \omega_z / P$ is presented as a function of the normalized distance x / h from the point of the application of the load P for two Poisson's ratios (top, $\nu = 0$; bottom, $\nu = 0.49$) and two different boundary conditions at the interface: either $\omega_z(x, h) = 0$ (left) or $m_{yz}(x, h) = 0$ (right). The classical elasticity solution for the layer of thickness h is superimposed.

In the case of couple-stress elasticity the displacement components and the rotation at the surface depend upon both the Poisson's ratio and the normalized length h/ℓ . For fixed layer thickness h and increasing ℓ or increasing Poisson's ratio the layer becomes stiffer. In fact it can be seen that both ℓ and ν play an important role in the qualitative characteristics of the behavior of the layer's surface. Note that in all the cases the classical elasticity layer solution is added. In general all the significant variations are observed in a region that extends about $x/h \approx 2$ laterally to the point of the application of the load and the gradient effects become important for decreasing h/ℓ — a stiffer layer can be obtained by reducing the thickness h or increasing the microstructural length ℓ . Furthermore, for increasing ℓ and decreasing ν the deformation field is rather confined to a region near the point of application of the load and the effect of the boundary conditions becomes significant as ℓ increases compared to the layer thickness.

Moving further from the point of the application of the load the effect of the rotation gradients gradually diminishes and the results regarding all the measured quantities converge to those of classical elasticity. In fact for increasing h/ℓ ratio the region of significance of the effect of the rotation gradients, in terms of x/h , decreases. It is concluded that for $h \geq 50\ell$ the displacements and the rotation have essentially

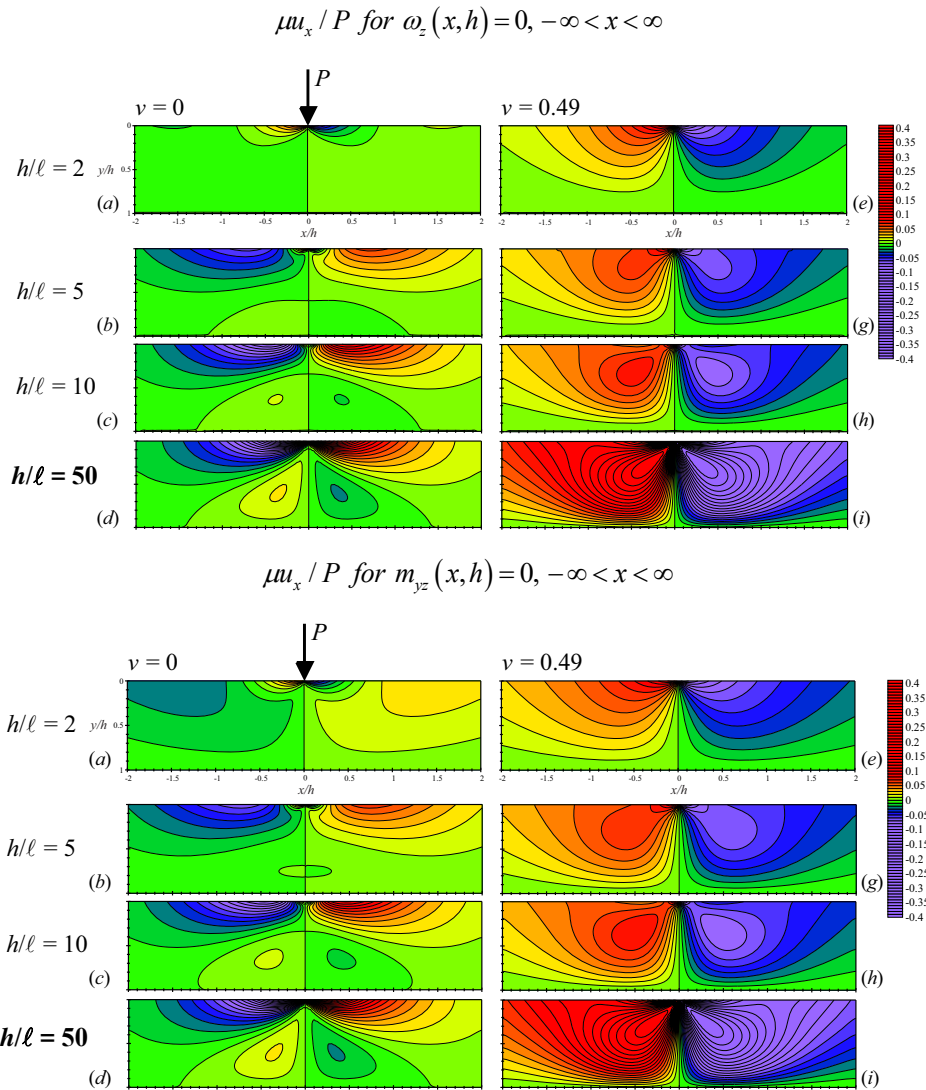


Figure 6. Contour fields of the normalized displacements $\mu u_x / P$ for different ratios h/ℓ and Poisson's ratios $\nu = 0$ and $\nu = 0.49$ in the frame of couple stress elasticity for $\omega_z(x, h) = 0$ and $m_{yz}(x, h) = 0$ at the interface. For increasing ℓ and decreasing ν the deformation field is confined to the region near the point of the application of the load.

converged to those obtained by classical elasticity excluding of course the singular behavior of the rotation observed in classical elasticity.

Next we examine the stress, couple stress and rotation fields at $y = h$ (that is the interface between the layer and the rigid substrate). The two different boundary conditions discussed previously are again considered and when $m_{yz} = 0$ we present the variation of the conjugate ω_z along the interface. The results are shown for selected values of Poisson's ratio ($\nu = 0$ and $\nu = 0.49$). For $\nu = 0$ and $\omega_z(x, h) = 0$ the

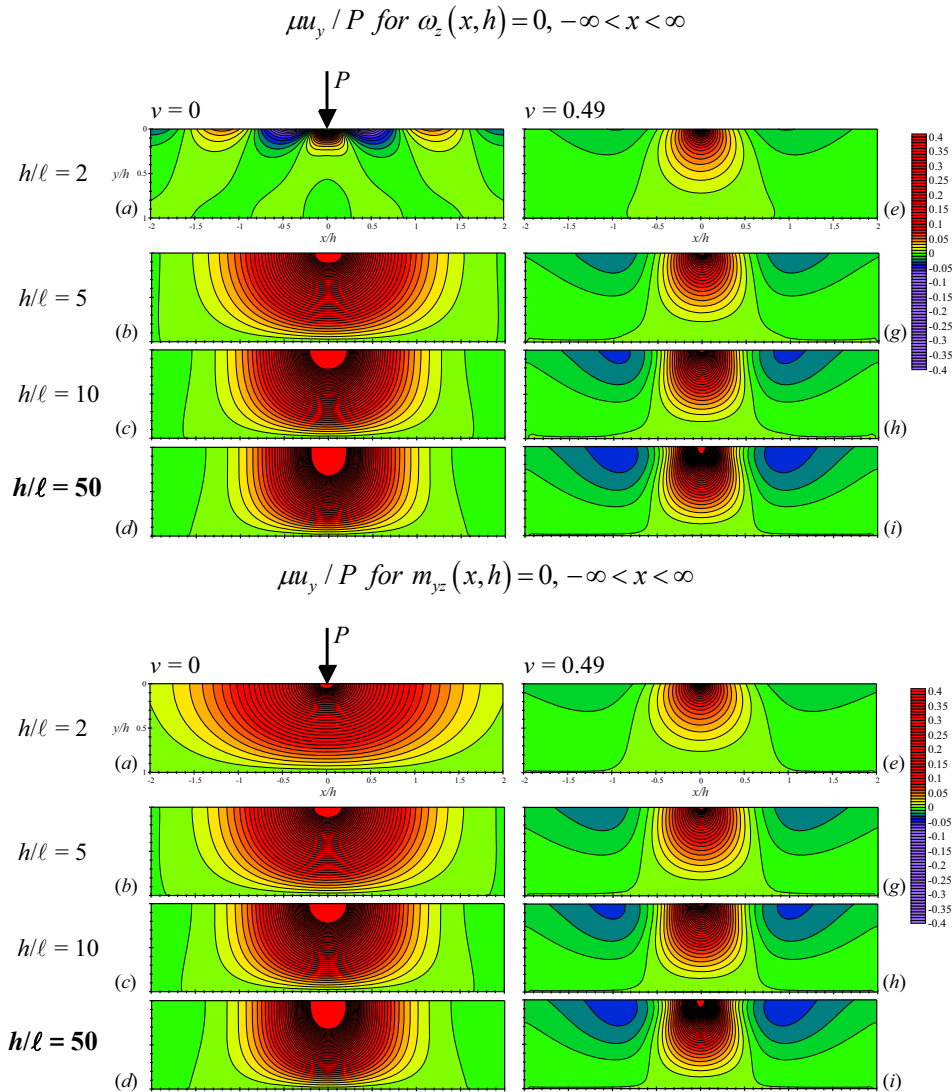


Figure 7. Contour fields of the normalized displacements $\mu u_y / P$ for different ratios h/ℓ and Poisson's ratios $\nu = 0$ and $\nu = 0.49$ in the frame of couple stress elasticity for $\omega_z(x, h) = 0$ and $m_{yz}(x, h) = 0$ at the interface.

normal stresses decrease for decreasing h/ℓ , everywhere along the interface are compressive and their peak values are bounded by the corresponding normal stresses obtained from classical elasticity. The shear stresses σ_{yx} are found decreased (at the region $-1 \leq x/h \leq 1$) compared to those that correspond to classical elasticity and at fixed x/h change sign for decreasing h/ℓ . Furthermore, m_{yz} decreases for increasing h/ℓ . For increasing Poisson's ratio all the stresses and couple-stresses increase and become higher than those obtained by classical elasticity theory. Furthermore, for decreasing h/ℓ and increasing Poisson's ratio the normal stresses become tensile at $1 \leq x/h \leq 2$ from the point of the application of

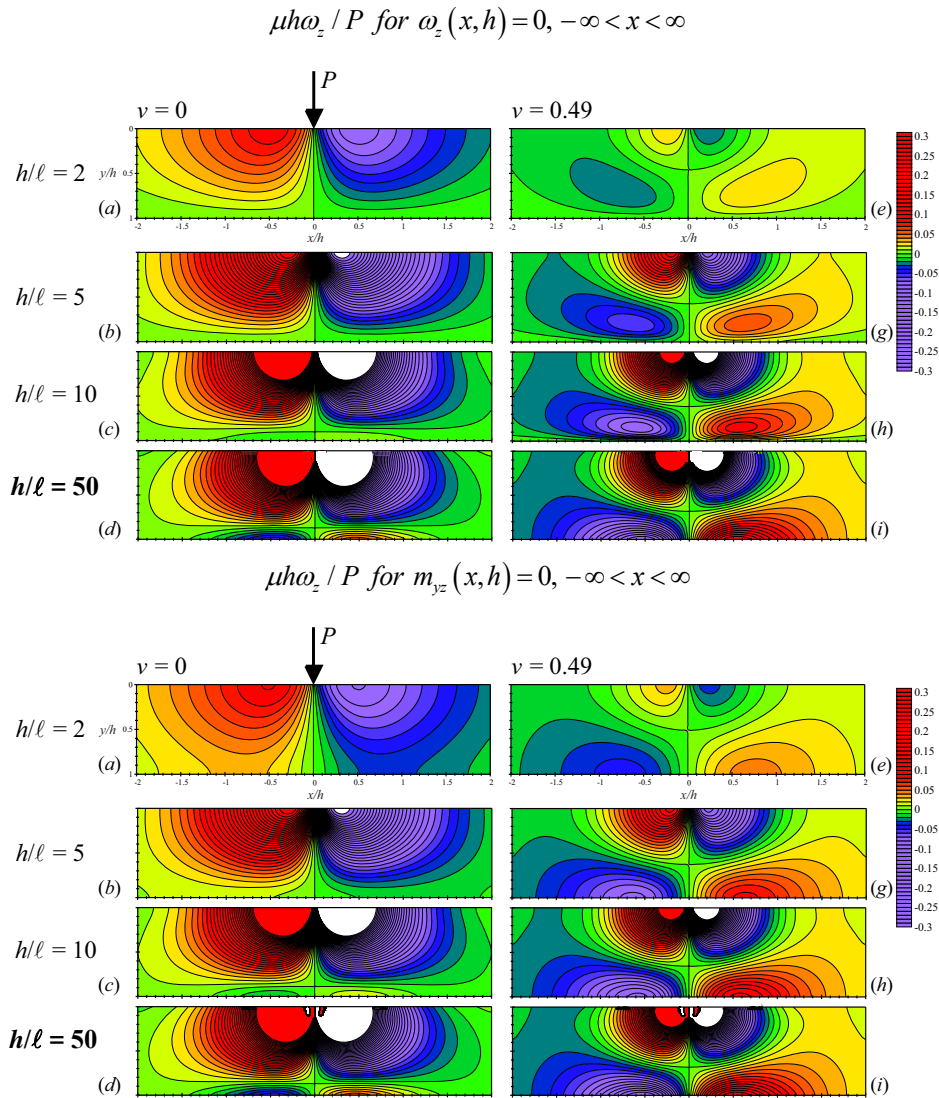


Figure 8. Contour fields of the normalized rotation $\mu h \omega_z / P$ for different ratios h/ℓ and Poisson's ratios $\nu = 0$ and $\nu = 0.49$ in the frame of couple stress elasticity for $\omega_z(x, h) = 0$ and $m_{yz}(x, h) = 0$ at the interface. The white region indicates $\mu h \omega_z / P < -0.3$.

the load. Finally, this region of tensile stresses vanishes for $m_{yz}(x, h) = 0$ instead of $\omega_z(x, h) = 0$ at $\nu = 0.49$.

We further note that bounded rotations have been found in both static as well as dynamic problems for concentrated loads in the context of the anisotropic couple-stress elasticity (see [Gourgiotis and Bigoni 2016; 2017] while similar results, in terms of rotations, have been observed in problems involving cracks within the same theory [Gourgiotis 2017; Mishuris et al. 2012; Morini et al. 2013; 2014; Piccolroaz et al.

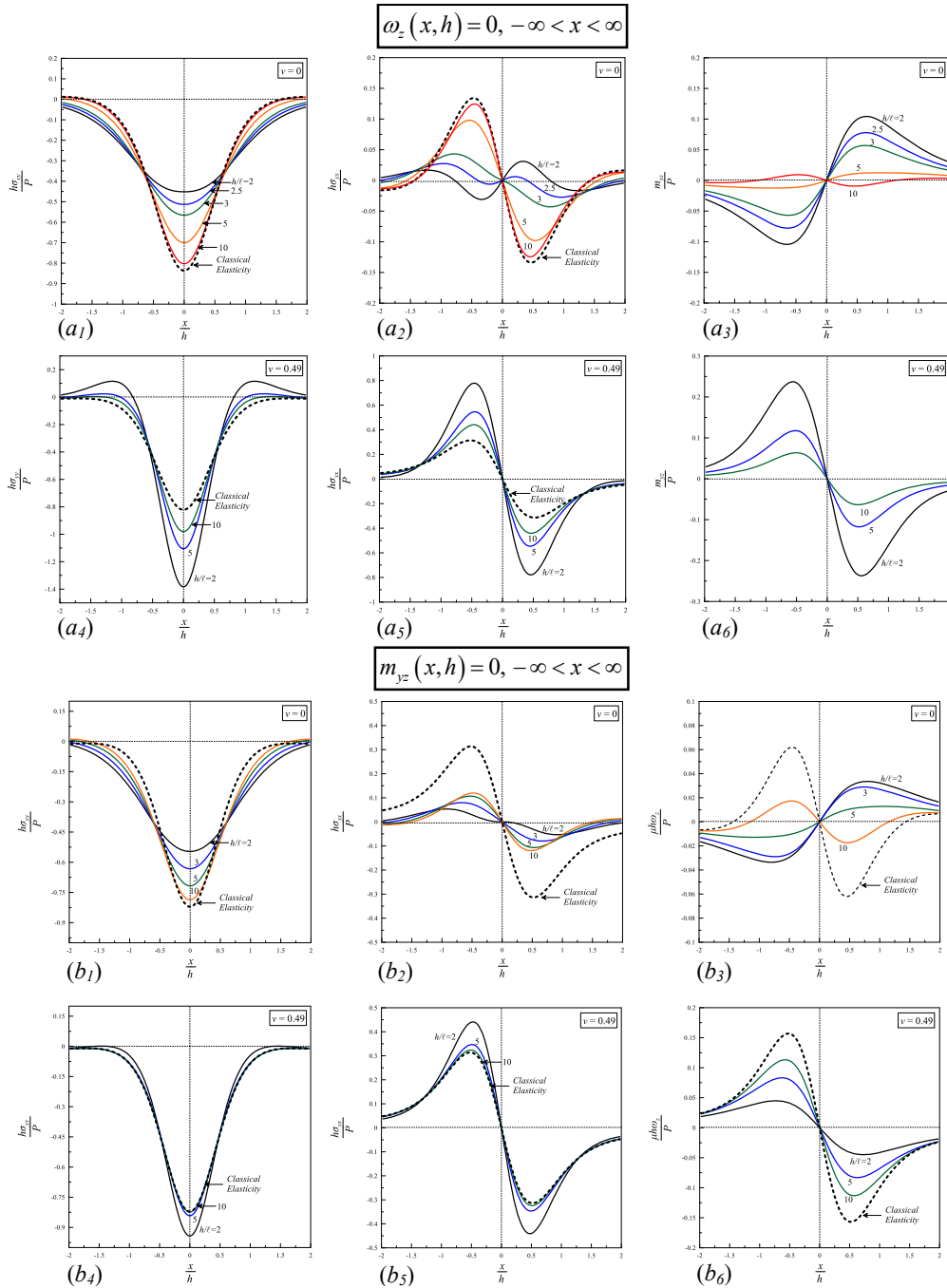


Figure 9. Normalized stress (σ_{yy} , σ_{yx}), couple stress (m_{yz}) or rotation (ω_z) distributions along the interface between the layer and the rigid substrate ($y = h$) in the frame of couple stress elasticity. Results are presented for the two different boundary conditions at the interface, $\omega_z(x, h) = 0$ (top) and $m_{yz}(x, h) = 0$ (bottom). The effect of Poisson's ratio is also shown for $\nu = 0$ and $\nu = 0.49$. The classical elasticity results are superimposed.

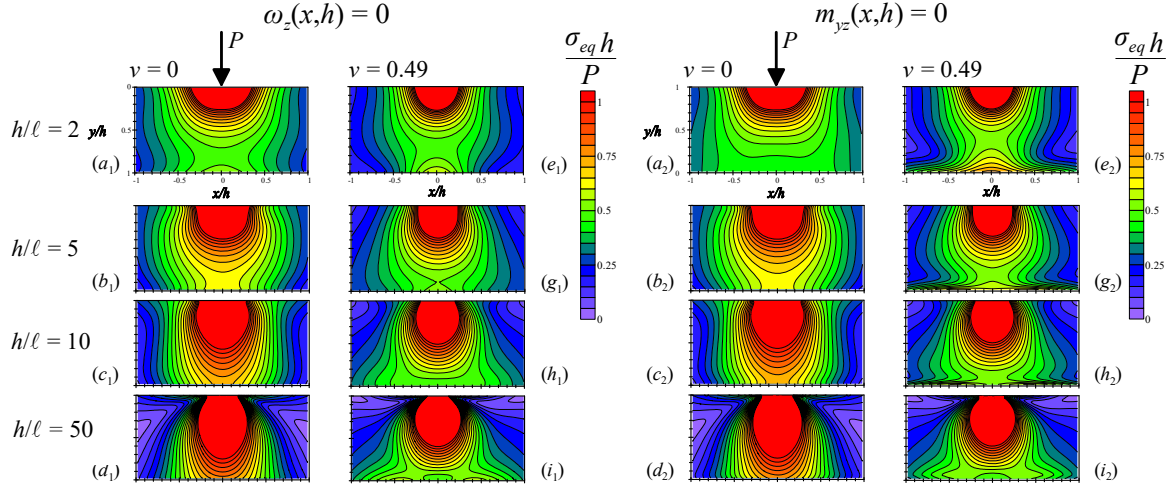


Figure 10. Contours of normalized equivalent stress $\sigma_{eq}h/P$ for different ratios h/ℓ . Results are presented for the two different boundary conditions at the interface, $\omega_z(x, h) = 0$ (left) and $m_{yz}(x, h) = 0$ (right). The effect of Poisson's ratio is also shown for $\nu = 0$ and $\nu = 0.49$.

2012; Radi 2008]. It should be further underlined that in contrast to concentrated load problems in the frame of the antiplane couple stress formulation, which predict bounded displacements as well as bounded strains at the point of the application of the load, here, in the plane strain formulation, both normal displacements as well as strains are in fact unbounded [Gourgiotis and Bigoni 2016; 2017; Zisis 2017]. Bounded strains have been found in Mode III cracks in the context of couple stress elasticity [Mishuris et al. 2012; Morini et al. 2013; 2014; Piccolroaz et al. 2012; Radi 2008].

It is also instructive to examine the equivalent stress in order to identify the severest stress state and accordingly the potential regions with respect to the point of the application of the load, that plasticity may emanate. In the context of couple stress theory the shape of the equivalent stress contours depends upon the microstructural characteristics of the material. For the case of couple stress elasticity and according to J_2 -flow theory, following [de Borst 1993] and [Shu and Fleck 1998], we introduce a general form of the normalized equivalent stress as:

$$\sigma_{eq} = \sqrt{3 \left(\frac{1}{2} (s_{xx}^2 + s_{yy}^2 + s_{zz}^2) + \frac{1}{4} \sigma_{xy}^2 + \frac{1}{2} \sigma_{xy} \sigma_{yx} + \frac{1}{4} \sigma_{yx}^2 + \frac{1}{2} \ell^2 (m_{xz}^2 + m_{yz}^2) \right)}, \quad (62)$$

where $s_{ij} = \sigma_{ij} - \frac{1}{3} \delta_{ij} \sigma_{kk}$ is the deviatoric stress.

When the equivalent stress reaches the material yield stress, yielding will commence — although the plastic enclave will be surrounded by elastic material — and at loads modestly above the elastic limit might be approximated in shape by one of the contours in Figure 10 depending upon the microstructural characteristic length ℓ and the Poisson's ratio ν assuming fixed layer thickness h . It is observed that for decreasing ℓ the maximum equivalent stress increases and the region of maximum equivalent stress expands vertically while it rather shrinks horizontally. For $\ell \rightarrow 0$ ($h/\ell \rightarrow \infty$, the classical elasticity solution), the maximum of the equivalent stress is shifted inside the layer and the potential yielding

region increases substantially almost reaching the interface between the layer and the rigid substrate. The effect of the boundary conditions at the interface upon the equivalent stress is also shown. As a final comment we note that classical elasticity suggest that at the surface of the layer or the half-plane the equivalent stress vanish. It can be seen from Figure 10 that this is not true for the case of couple stress elasticity due to the fact that as $y \rightarrow 0$, σ_{xx} , σ_{xy} and m_{xz} need not necessarily vanish. It is concluded that in order to avoid extensive plastic regions within the layer the ratio h/ℓ should be kept as low as possible, and the Poisson's ratio should be increased.

5. Conclusions

In the present work we examined the behavior of a microstructured layer bonded on a rigid substrate, under the action of a point load on its surface. This is essentially an extended version of the classical Burmister's problem in the context of a generalized theory of elasticity.

We have shown that both displacements (tangential and normal) present the same asymptotic characteristics near the point of the application of the load for both classical as well couple stress elasticity and this is in fact true for the case of the half-plane as well as the case of the layer of finite thickness. Nevertheless, both the quantitative and qualitative characteristics of the displacements are strongly affected by the ratio h/ℓ and this is for the first time shown. Furthermore, the rotation at the point of the application of the load is bounded in the frame of couple stress elasticity while it is singular in the frame of classical elasticity. Furthermore, as h/ℓ varies, the rotation field is strongly affected. It is furthermore shown, that when $h/\ell \geq 50$ the classical elasticity solution adequately predicts the behavior of the layer and the microstructural effects are of minor importance.

The results are important for the construction and the solution of more complicated contact problems towards the understanding of experimental details involved in the indentation technique for the mechanical characterization of coatings and thin films. Furthermore, the present results shed light to contact problems that take place in structural engineering given that structures are founded in reinforced concrete footings or pads buried at relatively shallow depths beneath the ground surface and large scale contacts take place between the footings and the deformable ground.

As a final comment, we note that the present approach and results are applicable to systems in which the substrate is much stiffer than the layer. Such systems can be found, among other areas, in aerospace applications. For example during the *high temperature* erosion of thermal barrier coatings experimental findings suggest that the observed deformation of the substrate is confined compared to the columnar ceramic layer (zirconia 8% yttria stabilized) — see for example [Chen et al. 2003; Fleck and Zisis 2010; Zisis and Fleck 2010] as well as the references therein. On the other hand, there are systems that the substrate is less stiff than the layer. Such systems are among others, titanium nitride and diamond like carbon thin films deposited on aluminium substrates that are used in magnetic hard disk industry. In this case it is of great interest to present the corresponding solutions, in the context of couple stress elasticity, incorporating in addition to the deformable layer a deformable substrate. It is expected that, apart from ratio of the classical material properties, the ratio of the characteristic lengths will be important to the system response and cases where the layer is stiffer than the substrate can be evaluated. This is within our scope for a future work.

Appendix

System of eight linear equations for the solution of $B_i(\xi)$ and $C_i(\xi)$ with $i = 1, \dots, 4$. Depending upon the boundary conditions at the bottom of the layer we have (for $\xi \geq 0$):

(1) Vanishing displacements and rotations at the bottom of the layer:

$$\begin{pmatrix} -\xi^2 & -\xi^2 & -\xi^2 & -\xi^2 & -i\xi^2 & i\xi & i\xi^2 & i\xi \\ -\xi & -\gamma & \xi & \gamma & 0 & 0 & 0 & 0 \\ i\xi^2 & i\xi\gamma & -i\xi^2 & -i\xi\gamma & -\xi^2 & 0 & -\xi^2 & 0 \\ \frac{e^{-h\xi}\xi}{2\mu} & \frac{e^{-h\gamma}\gamma}{2\mu} & -\frac{e^{h\xi}\xi}{2\mu} & -\frac{e^{h\gamma}\gamma}{2\mu} & \frac{ie^{-h\xi}\xi}{2\mu} & -\frac{ie^{-h\xi}(2(1-\nu)-h\xi)}{2\mu} & \frac{ie^{h\xi}\xi}{2\mu} & \frac{ie^{h\xi}(2(1-\nu)+h\xi)}{2\mu} \\ -\frac{ie^{-h\xi}\xi}{2\mu} & -\frac{ie^{-h\gamma}\gamma}{2\mu} & -\frac{ie^{h\xi}\xi}{2\mu} & -\frac{ie^{h\gamma}\gamma}{2\mu} & \frac{e^{-h\xi}\xi}{2\mu} & \frac{e^{-h\xi}(1-2\nu+h\xi)}{2\mu} & -\frac{e^{h\xi}\xi}{2\mu} & \frac{e^{h\xi}(1-2\nu-h\xi)}{2\mu} \\ 0 & -\frac{e^{-h\gamma}}{4\ell^2\mu} & 0 & -\frac{e^{h\gamma}}{4\ell^2\mu} & 0 & \frac{ie^{-h\xi}(1-\nu)\xi}{\mu} & 0 & \frac{ie^{h\xi}(1-\nu)\xi}{\mu} \\ 1 & 0 & 0 & 0 & 0 & 4i\ell^2(1-\nu)\xi & 0 & 0 \\ 0 & 0 & 1 & 0 & 0 & 0 & 0 & 4i\ell^2(1-\nu)\xi \end{pmatrix} \begin{pmatrix} B_1(\xi) \\ B_2(\xi) \\ B_3(\xi) \\ B_4(\xi) \\ C_1(\xi) \\ C_2(\xi) \\ C_3(\xi) \\ C_4(\xi) \end{pmatrix} = \begin{pmatrix} 0 \\ 0 \\ P \\ 0 \\ 0 \\ 0 \\ 0 \\ 0 \end{pmatrix}$$

(2) Vanishing displacements and couple stresses at the bottom of the layer:

$$\begin{pmatrix} -\xi^2 & -\xi^2 & -\xi^2 & -\xi^2 & -i\xi^2 & i\xi & i\xi^2 & i\xi \\ -\xi & -\gamma & \xi & \gamma & 0 & 0 & 0 & 0 \\ i\xi^2 & i\xi\gamma & -i\xi^2 & -i\xi\gamma & -\xi^2 & 0 & -\xi^2 & 0 \\ \frac{e^{-h\xi}\xi}{2\mu} & \frac{e^{-h\gamma}\gamma}{2\mu} & -\frac{e^{h\xi}\xi}{2\mu} & -\frac{e^{h\gamma}\gamma}{2\mu} & \frac{ie^{-h\xi}\xi}{2\mu} & -\frac{ie^{-h\xi}(2(1-\nu)-h\xi)}{2\mu} & \frac{ie^{h\xi}\xi}{2\mu} & \frac{ie^{h\xi}(2(1-\nu)+h\xi)}{2\mu} \\ -\frac{ie^{-h\xi}\xi}{2\mu} & -\frac{ie^{-h\gamma}\gamma}{2\mu} & -\frac{ie^{h\xi}\xi}{2\mu} & -\frac{ie^{h\gamma}\gamma}{2\mu} & \frac{e^{-h\xi}\xi}{2\mu} & \frac{e^{-h\xi}(1-2\nu+h\xi)}{2\mu} & -\frac{e^{h\xi}\xi}{2\mu} & \frac{e^{h\xi}(1-2\nu-h\xi)}{2\mu} \\ -e^{-h\xi}\xi & -e^{-h\gamma}\gamma & e^{h\xi}\xi & e^{h\gamma}\gamma & 0 & 0 & 0 & 0 \\ 1 & 0 & 0 & 0 & 0 & 4i\ell^2(1-\nu)\xi & 0 & 0 \\ 0 & 0 & 1 & 0 & 0 & 0 & 0 & 4i\ell^2(1-\nu)\xi \end{pmatrix} \begin{pmatrix} B_1(\xi) \\ B_2(\xi) \\ B_3(\xi) \\ B_4(\xi) \\ C_1(\xi) \\ C_2(\xi) \\ C_3(\xi) \\ C_4(\xi) \end{pmatrix} = \begin{pmatrix} 0 \\ 0 \\ P \\ 0 \\ 0 \\ 0 \\ 0 \\ 0 \end{pmatrix}$$

where $\gamma \equiv \gamma(\xi) = (1/\ell^2 + \xi^2)^{1/2}$.

References

- [Bacca et al. 2013] M. Bacca, D. Bigoni, F. Dal Corso, and D. Veber, "Mindlin second-gradient elastic properties from dilute two-phase Cauchy-elastic composites, I: Closed form expression for the effective higher-order constitutive tensor", *Int. J. Solids Struct.* **50** (2013), 4010–4019.
- [Barber 2010] J. R. Barber, *Elasticity*, 3rd ed. ed., Solid mechanics and its applications **172**, Springer, 2010.
- [Begley and Hutchinson 1998] M. R. Begley and J. W. Hutchinson, "The mechanics of size-dependent indentation", *J. Mech. Phys. Solids* **46** (1998), 2049–2068.
- [Bigoni and Drugan 2007] D. Bigoni and W. J. Drugan, "Analytical derivation of cosserat moduli via homogenization of heterogeneous elastic materials", *J. Appl. Mech. (ASME)* **74** (2007), 741–753.
- [Biot 1935] M. A. Biot, "Effect of certain discontinuities on the pressure distribution in a loaded soil", *J. Appl. Phys.* **6**:12 (1935), 367–375.
- [de Borst 1993] R. de Borst, "A generalisation of J2-flow theory for polar continua", *Computer Methods Appl. Mech. Eng.* **103**:3 (1993), 347–362.
- [Burmister 1943] D. M. Burmister, "Theory of stress and displacement in layered system and applications to the design of airport", in *Proceedings of Annual Meeting of the Transportation Research Board*, Highway Research Board, Washington, DC, 1943.

- [Burmister 1945a] D. M. Burmister, “The general theory of stresses and displacements in layered systems, I”, *J. Appl. Phys.* **16**:2 (1945), 89–94.
- [Burmister 1945b] D. M. Burmister, “The general theory of stresses and displacements in layered soil systems, III”, *J. Appl. Phys.* **16**:5 (1945), 296–302.
- [Burmister 1956] D. M. Burmister, “Stress and displacement characteristics of a two-layer rigid base soil system: influence diagrams and practical applications”, *Proc. Highway Res. Board* **35** (1956), 773–814.
- [Burmister et al. 1944] D. M. Burmister, L. A. Palmer, E. S. Barber, and T. A. Middlebrooks, “The theory of stress and displacements in layered systems and applications to the design of airport runways”, *Highway Res. Board Proc.* **23** (1944), 126–148.
- [Chen et al. 1998] J. Y. Chen, Y. Huang, and M. Ortiz, “Fracture analysis of cellular materials: a strain gradient model”, *J. Mech. Phys. Solids* **46** (1998), 789–828.
- [Chen et al. 2003] X. Chen, R. Wang, N. Yao, A. G. Evans, J. W. Hutchinson, and R. W. Bruce, “Foreign object damage in a thermal barrier system: mechanisms and simulations”, *Mater. Sci. Eng. A* **352** (2003), 221.
- [Davis and Poulos 1963] E. H. Davis and H. G. Poulos, “Triaxial testing and three-dimensional settlement analysis”, research report, Peter Nicol Russell School of Civil Engineering, University of Sydney, 1963.
- [Davis and Taylor 1961] E. H. Davis and H. Taylor, “The surface displacement of an elastic layer due to horizontal and vertical surface loading”, pp. 621– in *Proc. 5th Intern. Conf. Soil Mechanics and Foundation Engineering* (Paris, 1961), vol. 1, Dunod, Paris, 1961.
- [Fleck and Zisis 2010] N. A. Fleck and T. Zisis, “The erosion of EB-PVD thermal barrier coatings: The competition between mechanisms”, *Wear* **268** (2010), 1214–1224.
- [Fung 1965] Y. C. Fung, *Foundations of solid mechanics*, Prentice-Hall, Englewood Cliffs, NJ, 1965.
- [Georgiadis and Anagnostou 2008] H. G. Georgiadis and D. S. Anagnostou, “Problems of the Flamant–Boussinesq and Kelvin type in dipolar gradient elasticity”, *J. Elasticity* **90** (2008), 71–98.
- [Gourgiotis 2017] P. A. Gourgiotis, “Shear crack growth in brittle materials modeled by constrained Cosserat elasticity”, *J. Eur. Ceram. Soc.* **38**:8 (2017), 3025–3036.
- [Gourgiotis and Bigoni 2016] P. A. Gourgiotis and D. Bigoni, “Stress channelling in extreme couple-stress materials Part I: Strong ellipticity, wave propagation, ellipticity, and discontinuity relations”, *J. Mech. Phys. Solids* **88** (2016), 150–168.
- [Gourgiotis and Bigoni 2017] P. A. Gourgiotis and D. Bigoni, “The dynamics of folding instability in a constrained Cosserat medium”, *Phil. Trans. R. Soc. A* **375**:2093 (2017), 20160159.
- [Gourgiotis and Piccolroaz 2014] P. A. Gourgiotis and A. Piccolroaz, “Steady-state propagation of a Mode II crack in couple stress elasticity”, *Int. J. Fract.* **188** (2014), 119–145.
- [Gourgiotis and Zisis 2016] P. Gourgiotis and T. Zisis, “Two-dimensional indentation of microstructured solids characterized by couple-stress elasticity”, *J. Strain Anal. Eng. Des.* **51**:4 (2016), 318–331.
- [Gourgiotis et al. 2018] P. A. Gourgiotis, T. Zisis, and H. G. Georgiadis, “On concentrated surface loads and Green’s functions in the Toupin–Mindlin theory of strain-gradient elasticity”, *Int. J. Solids Struct.* **130** (2018), 153–171.
- [Green and Zerna 1968] A. E. Green and W. Zerna, *Theoretical elasticity*, Oxford University Press, Oxford, 1968.
- [Hills and Nowell 1994] D. Hills and D. Nowell, *Mechanics of fretting fatigue*, Kluwer, Dordrecht, 1994.
- [Johnson 1985] K. Johnson, *Contact mechanics*, Cambridge University Press, Cambridge, UK, 1985.
- [Koiter 1964a] W. T. Koiter, “Couple stresses in the theory of elasticity, I”, *Proc. Kon. Nederl. Akad. Wetensch. B* **67** (1964), 17–29.
- [Koiter 1964b] W. T. Koiter, “Couple stresses in the theory of elasticity, II”, *Proc. Kon. Nederl. Akad. Wetensch. B* **67** (1964), 30–44.
- [Love 1952] A. E. H. Love, *A treatise on the mathematical theory of elasticity*, Cambridge University Press, New York, 1952.
- [Maranganti and Sharma 2007] R. Maranganti and P. Sharma, “A novel atomistic approach to determine strain-gradient elasticity constants: Tabulation and comparison for various metals, semiconductors, silica, polymers and the (Ir) relevance for nanotechnologies”, *J. Mech. Phys. Solids* **55** (2007), 1823–1852.

- [Marguerre 1931] K. Marguerre, "Druckverteilung durch eine elastische Schicht auf starrer rauher Unterlage", *Arch. Appl. Mech.* **2**:1 (1931), 108–117.
- [Mindlin 1963] R. D. Mindlin, "Influence of couple-stresses on stress concentrations", *Experim. Mech.* **3**:1 (1963), 1–7.
- [Mindlin and Tiersten 1962] R. D. Mindlin and H. F. Tiersten, "Effects of couple-stresses in linear elasticity", *Arch. Ration. Mech. Anal.* **11** (1962), 415–448.
- [Mishuris et al. 2012] G. Mishuris, A. Piccolroaz, and E. Radi, "Steady-state propagation of a Mode III crack in couple stress elastic materials", *Int. J. Eng. Sci.* **61** (2012), 112–128.
- [Morini et al. 2013] L. Morini, A. Piccolroaz, G. Mishuris, and E. Radi, "On fracture criteria for dynamic crack propagation in elastic materials with couple stresses", *Int. J. Eng. Sci.* **71** (2013), 45–61.
- [Morini et al. 2014] L. Morini, A. Piccolroaz, and G. Mishuris, "Remarks on the energy release rate for an antiplane moving crack in couple stress elasticity", *Int. J. Solids Struct.* **51**:18 (2014), 3087–3100.
- [Muki and Sternberg 1965] R. Muki and E. Sternberg, "The influence of couple-stresses on singular stress concentrations in elastic solids", *Z. Angew. Math. Phys.* **16** (1965), 611–648.
- [Nix and Gao 1998] W. D. Nix and H. Gao, "Indentation size effects in crystalline materials: a law for strain gradient plasticity", *J. Mech. Phys. Solids* **46** (1998), 411–425.
- [Piccolroaz et al. 2012] A. Piccolroaz, G. Mishuris, and E. Radi, "Mode III interfacial crack in the presence of couple stress elastic materials", *Eng. Fract. Mech.* **80**:1 (2012), 60–71.
- [Pickett 1938] G. Pickett, pp. 35–47 in *Proc. Highw. Res. Board*, vol. 18, 1938.
- [Poole et al. 1996] W. J. Poole, M. F. Ashby, and N. A. Fleck, "Micro-hardness of annealed and work-hardened copper polycrystals", *Scr. Mater.* **34** (1996), 559–564.
- [Poulos 1967] H. G. Poulos, "Stresses and displacements in an elastic layer underlain by a rough rigid base", *Géotechnique* **17**:4 (1967), 378–410.
- [Radi 2008] E. Radi, "On the effects of the characteristic lengths in bending and torsion on Mode III crack in couple stress elasticity", *Int. J. Solids Struct.* **45**:10 (2008), 3033–3058.
- [Schiffman 1957] R. L. Schiffman, "The numerical solution for stresses and displacements in a three-layer soil system", pp. 169–173 in *Proceedings of the 4th International Conference on Soil Mechanics and Foundation Engineering*, vol. 2, 1957.
- [Shodja et al. 2013] H. M. Shodja, A. Zaheri, and A. Tehranchi, "Ab initio calculations of characteristic lengths of crystalline materials in first strain gradient elasticity", *Mech. Mater.* **61** (2013), 73–78.
- [Shu and Fleck 1998] J. Y. Shu and N. A. Fleck, "The prediction of a size effect in microindentation", *Int. J. Solids Struct.* **35** (1998), 1363–1383.
- [Tekoglu and Onck 2008] C. Tekoglu and P. R. Onck, "Size effect in two dimensional Voronoi foams. A comparison between generalized continua and discrete models", *J. Mech. Phys. Solids* **56** (2008), 3541–3564.
- [Timoshenko and Goodier 1970] S. P. Timoshenko and J. N. Goodier, *Theory of elasticity*, McGraw-Hill, New York, 1970.
- [Toupin 1964] R. A. Toupin, "Theories of elasticity with couple-stress", *Arch. Ration. Mech. Anal.* **17** (1964), 85–112.
- [Wei and Hutchinson 2003] Y. Wei and J. W. Hutchinson, "Hardness trends in micron scale indentation", *J. Mech. Phys. Solids* **51** (2003), 2037–2056.
- [Zisis 2017] T. Zisis, "Anti-plane loading of microstructured materials in the context of couple stress theory of elasticity: half-planes and layers", *Arch. Appl. Mech.* (2017), 1–14.
- [Zisis and Fleck 2010] T. Zisis and N. A. Fleck, "The elastic-plastic indentation response of a columnar thermal barrier coating", *Wear* **268** (2010), 443–454.
- [Zisis et al. 2014] T. Zisis, P. A. Gougiotis, K. P. Baxevanakis, and H. G. Georgiadis, "Some basic contact problems in couple-stress elasticity", *Int. J. Solids Struct.* **51** (2014), 2084–2095.

Received 31 Jan 2018. Revised 13 Mar 2018. Accepted 19 Mar 2018.

THANASIS ZISIS: zisis@mail.ntua.gr

Mechanics Division, National Technical University of Athens, Athens, Greece

JOURNAL OF MECHANICS OF MATERIALS AND STRUCTURES

msp.org/jomms

Founded by Charles R. Steele and Marie-Louise Steele

EDITORIAL BOARD

ADAIR R. AGUIAR	University of São Paulo at São Carlos, Brazil
KATIA BERTOLDI	Harvard University, USA
DAVIDE BIGONI	University of Trento, Italy
MAENGHYO CHO	Seoul National University, Korea
HUILING DUAN	Beijing University
YIBIN FU	Keele University, UK
IWONA JASIUKEWICZ	University of Illinois at Urbana-Champaign, USA
DENNIS KOCHMANN	ETH Zurich
MITSUTOSHI KURODA	Yamagata University, Japan
CHEE W. LIM	City University of Hong Kong
ZISHUN LIU	Xi'an Jiaotong University, China
THOMAS J. PENCE	Michigan State University, USA
GIANNI ROYER-CARFAGNI	Università degli studi di Parma, Italy
DAVID STEIGMANN	University of California at Berkeley, USA
PAUL STEINMANN	Friedrich-Alexander-Universität Erlangen-Nürnberg, Germany
KENJIRO TERADA	Tohoku University, Japan

ADVISORY BOARD

J. P. CARTER	University of Sydney, Australia
D. H. HODGES	Georgia Institute of Technology, USA
J. HUTCHINSON	Harvard University, USA
D. PAMPLONA	Universidade Católica do Rio de Janeiro, Brazil
M. B. RUBIN	Technion, Haifa, Israel

PRODUCTION production@msp.org

SILVIO LEVY Scientific Editor

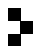
Cover photo: Mando Gomez, www.mandolux.com

See msp.org/jomms for submission guidelines.

JoMMS (ISSN 1559-3959) at Mathematical Sciences Publishers, 798 Evans Hall #6840, c/o University of California, Berkeley, CA 94720-3840, is published in 10 issues a year. The subscription price for 2018 is US \$615/year for the electronic version, and \$775/year (+\$60, if shipping outside the US) for print and electronic. Subscriptions, requests for back issues, and changes of address should be sent to MSP.

JoMMS peer-review and production is managed by EditFLOW[®] from Mathematical Sciences Publishers.

PUBLISHED BY

 **mathematical sciences publishers**
nonprofit scientific publishing

<http://msp.org/>

© 2018 Mathematical Sciences Publishers

Journal of Mechanics of Materials and Structures

Volume 13, No. 2

March 2018

- A simple technique for estimation of mixed mode (I/II) stress intensity factors**
SOMAN SAJITH, KONDEPUDI S.R.K. MURTHY and PUTHUVEETIL S. ROBI 141
- Longitudinal shear behavior of composites with unidirectional periodic nanofibers of some regular polygonal shapes**
HAI-BING YANG, CHENG HUANG, CHUAN-BIN YU and CUN-FA GAO 155
- Fracture initiation in a transversely isotropic solid: transient three dimensional analysis**
LOUIS M. BROCK 171
- Eshelby inclusion of arbitrary shape in isotropic elastic materials with a parabolic boundary**
XU WANG, LIANG CHEN and PETER SCHIAVONE 191
- Burmister's problem extended to a microstructured layer**
THANASIS ZISIS 203
- Multiple crack damage detection of structures using simplified PZT model**
NARAYANAN JINESH and KRISHNAPILLAI SHANKAR 225



1559-3959(2018)13:2;1-#